1-1-2015

Evaluation Of Mems Fabricated Fractal Based Free Standing Scaffolds For The Purposes Of Developing A Brain Bioreactor

Brandy Broadbent
Wayne State University,

EVALUATION OF MEMS FABRICATED FRACTAL BASED FREE STANDING SCAFFOLDS FOR THE PURPOSES OF DEVELOPING A BRAIN BIOREACTOR

by

BRANDY BROADBENT

THESIS

Submitted to the Graduate School

of Wayne State University,

Detroit, Michigan

in partial fulfillment of the requirements

for the degree of

MASTER OF SCIENCE

2015

MAJOR: BIOMEDICAL ENGINEERING

Approved By:

_____

Advisor Date

DEDICATION

I would like to dedicate this thesis to my loving and encouraging family. First to my parents, Don and Maxanna Lucas, who listened diligently and patiently to the many challenges I encountered during this work and always assured me that I would be successful in meeting the challenges associated with painstaking research. Second to my girls, Mikayla and Elise Broadbent, who provided a much needed distraction on nights and weekends and prevented me from becoming too consumed with my studies. Finally, to my husband, William Broadbent, for being open to me embarking on a new path and pursing my love of science and engineering.

ACKNOWLEDGEMENTS

I would like to give my sincere appreciation to the members of the Smart Sensors and Integrated Microsystems Lab and the members of Dr. John Cavanaugh's lab. I am very thankful to Barb House who gave me much of her time to show me how to navigate the university ordering system and helped me track down misplaced orders before they spoiled. I am very appreciative to Tara Twomey for lending me her expertise in cell culture techniques and guiding me through trouble shooting methods during the multiple challenges I encountered. I would also like to thank I would also like to thank Dr. Rachel Kast for her constant mentorship, encouragement, brainstorming sessions, and tutelage in statistics and SPSS software. I would also like to thank Dr. John Cavanaugh for allowing me to begin research in his lab and learn several of the techniques that were critical to completing this thesis. Finally I would like to thank Dr. Gregory Auner for the opportunity to work in a laboratory with many diverse opportunities and experts in a wide variety of fields. This thesis would not be possible without his mentorship and generous financial support.

TABLE OF CONTENTS

LIST OF TABLES

LIST OF FIGURES

CHAPTER 1 - NEURAL TISSUE ENGINEERING

1.1 - Background

The mammal central nervous system (CNS) is quite different from other organs in the body in that it lacks the ability to regenerate in a significant manner. The modest function that is regained after an injury is usually due to the plasticity in the neurons that allows them to reroute and make up for the injured neurons [1]. There are three types of limited regeneration that can occur in neurons. First, a peripheral nerve in the CNS (or in the peripheral nervous system) can regrow the distal end of an axon if is severed. This injury is most successfully treated when it is a sensory or motor nerve that is damaged [1]. The second type of regeneration in the CNS is extremely modest. It is possible for injured nerve cells to regrow and make new connections; however this is done on a very limited base due to the scaring from a significant increase in glial cells that inhibit neuron growth [1]. The third type of repair is for the CNS to create new neurons from stem cells [1]. Thus far, only the olfactory bulb and hippocampus have been identified as being able to create new neurons, however the majority of these neurons die before being integrated into the CNS [1]. Given the extremely limited ability of the CNS to repair itself, neurological disorders and injury exact a heavy toll on the people across the world.

Disorders or injury of the CNS can include Alzheimer's, Parkinson's, Huntington's, epilepsy, traumatic brain injury (TBI), and partial or complete damage to the spinal cord. Regarding neurological disorders, the World Health Organization reported in 2007 that worldwide, up to one billion people suffer from neurological disorders [2]. Epilepsy and Alzheimer's (including other dementias) contribute heavily

to that figure with 50 million and 24 million people afflicted, respectively [2]. Neurological disorders have a significant negative impact on the quality of life for those affected and require much support from their friends, family, and medical community.

In addition to neurological disorders, injury to the spinal cord resulting in paraplegia and tetraplegia are exceptionally debilitating to thousands of people. According to the National Spinal Cord Injury Statistical Center, there are 12,000 new cases of spinal cord injuries (SCI) in the United States per year, with approximately 273,000 people living with a SCI [3]. Of note, the average life expectancy of someone who has incurred a SCI is sixteen and a half years less, on average, than someone who has no injury; and this number has not improved since the 1980's [3]. Given the limited ability for the CNS to repair itself and the prevalence of neurological disorders and injuries to the CNS, there is a critical need to improve treatment capabilities.

Improved implant devices are needed in order to improve treatment of both neurological disorders and CNS injuries. A proper implant device can be integrated with electrical stimulation to try and return functionality as in the case with some neurological disorders or help to efficiently guide neurons to find other available neurons to connect as is the case with SCI [4]. Currently, treatment methods for neurological disorders and SCI do not rehabilitate patients to their pre-disorder/injury condition, but they are improving. In treatment for neurological movement disorders such as Parkinson's, Huntington's, and epilepsy, deep brain stimulation (DBS) is used by implanting microelectrode arrays in the patient. Implant devices also have a crucial role in caring for CNS injuries. One treatment for SCI is using an implanted device that can serve to facilitate growth of

neurons in an attempt to regain function of the spinal cord and affected limbs. One problem in directing the growth of neurons in the CNS is that they tend to scatter and they do not usually extend past the implant device and enter the host tissue [5]. The majority of scaffolds used to try and graft nerves are linear rather than use topology found in the body [6]. Scaffolds based on fractal design could improve neuronal growth by offering more areas for the nerves to connect to each other.

Fractals serve an important role in nature and in biomedical devices. Fractals are objects that have self-similarity at every level of magnification; when the object is scaled up or scaled down it remains the same [7]. There are many examples of fractals that occur naturally including coast lines, branching in trees, lungs, the vascular system, and the cortex. Fractals offer an advantage in the surface area to volume ratio over other geometries. For example, if the alveoli in the lungs were laid out flat, they would occupy an entire tennis court [8]. However, due to their fractal geometry which provides a high surface area to volume ratio, they reside in the relatively small space of the thoracic cavity.

There is also fractal geometry present in the brain. On a macro-scale, the human cortex exhibits self-similarity. In a study done using fast Fourier transformation, researchers found that the cortex has a fractal dimension of 2.80 when analyzed from the whole cortex down to 3 millimeters [9]. The cortex has two dimensions, length and width, so it is considered a plane [10]. It is folded into a self-similar pattern that maximizes surface area and in a limited amount of volume. The fractal dimension of 2.80 +/- .05 indicates that, because of the complexity of the cortex, it occupies space

almost as if it has a volume with three dimensions [10]. Fractal dimensions have also been calculated for neurons. For example, ganglia neurons have a fractal dimension of approximately 1.55 [11]. The dendrites of a neuron are similar to a line, which has a dimension of one, so a fractal dimension greater than one but less than two gives an indication of the complexity of the dendrite [11]. On the micro-scale, it is important to understand the morphology and geometry of neurons in order to better predict how they might grow and establish neural networks.

In addition, fractal geometry also offers structural stability through repeated patterns. The use of fractals in tissue engineering research is relatively new, beginning to accelerate in 2006 [12]. Using fractals in tissue engineering and implant devices could lead to designs that have improved biomimicry by capturing some of the complexity found in geometries in the body. Creating a fractal pattern on the surface used to grow cells, including cancer cells and neurons, has shown to provide an advantage to the cells growth and motility due to the increase in surface area [12]. Using fractals in tissue engineering and regenerative medicine is promising and scaffolds or implant devices using fractal geometry could potentially encourage greater cell growth by offering more surface area for the

The brain is the most complex organ in the human body with billions of neuronal connections and a variety of cells types and neurotransmitters [13]. In part due to its complexity and in part due to limited instruments to study the brain, there are several neurodegenerative diseases, to include Alzheimer's (AD) and Parkinson's (PD), that are not well understood and this limits treatments available for these patients. Although

animal models are typically used to study neurodegenerative diseases, there are limitations for what can be studied. For example, over 90% of patients who develop AD do so with no genetic predisposition to AD, however mice models are transfected by genes that cause AD, thus excluding the majority of AD cases from study [14]. The underlying cause of PD is also not well understood, for similar reasons. In order to study PD in animal models, researchers use neurotoxins to induce PD like symptoms, however it is unclear if the mechanism behind the drugs is the same as the disease [14]. Researchers use a variety of animals to study neurodegenerative disease to include rats, mice, zebra fish, drosophila, and *c. elegans* and while these models have provided valuable information, their nervous system is different and, in the case of the non-mammalians, far more simple than the human nervous system [15]. The development of a more human like model of the brain could assist researchers in determining the etymologies of neurodegenerative diseases. To this end, a brain bioreactor could provide more accurate information than animal models about mechanisms of disease and effects of drug treatments. Although the ultimate goal of developing a brain bioreactor would employ the use of human stem cells, at this point in development E18 Sprague Dawley rat neurons were used in scaffold testing.

Neural tissue engineering is a relatively new field and can improve the way drugs are tested, help repair damaged parts of the brain, and provide a more realistic platform to study the brain. The development of a bioreactor that is capable of supporting multiple neuronal cell types and provides for long term viability of cells for testing and observation is necessary to assist in understanding of the brain and in development of

drugs to treat diseases affecting the brain such as mental illness and neurodegenerative disease. There are many challenges to engineering a neuronal bioreactor; some of the challenges that will be addressed in this manuscript include identifying a biocompatible material, selecting a scaffold, directing neuron placement and outgrowths, and long term viability.

There is current research into neuronal bioreactors using different approaches including MEMs technology, microfluidics, digital sculpting, and gels. An optimized bioreactor would have architecture similar to the brain, induce 3D growth of the neural cells, and provide fresh media for long term cell culture. Each of these goals has unique challenges. The following will outline three different scaffolds designed for neural tissue engineering. The development of an exclusively MicroElectroMechanical system (MEMs) scaffold was designed by Rowe et al with the use of SU-8 and a grid like pattern, figure 1 [16]. This microscaffold structure incorporated channels to provide fresh media for the cells and electrodes to stimulate neurons [16]. The neurons grew on the scaffold, but it does appear that the neurons were prone to clumping.

A.

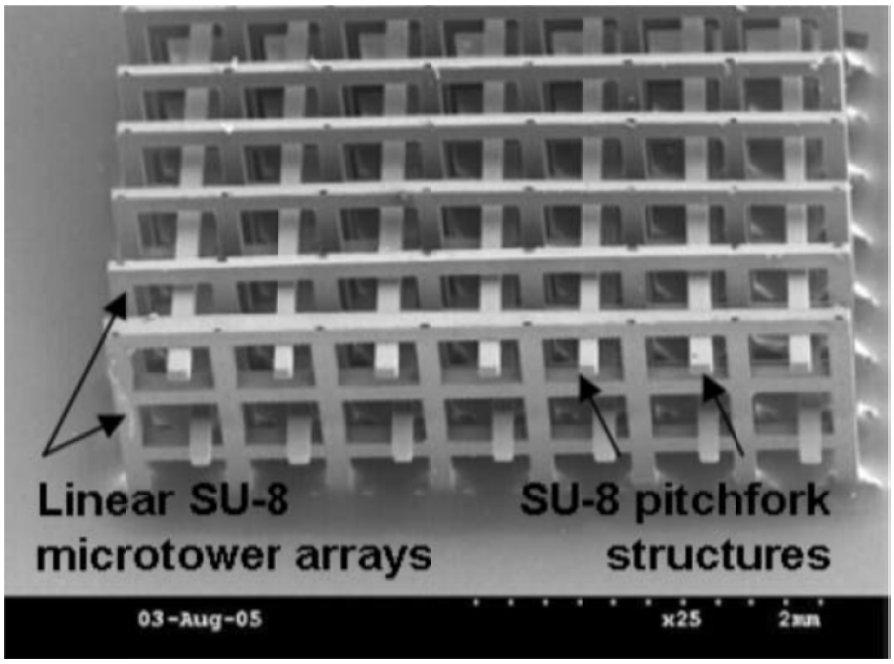

B.

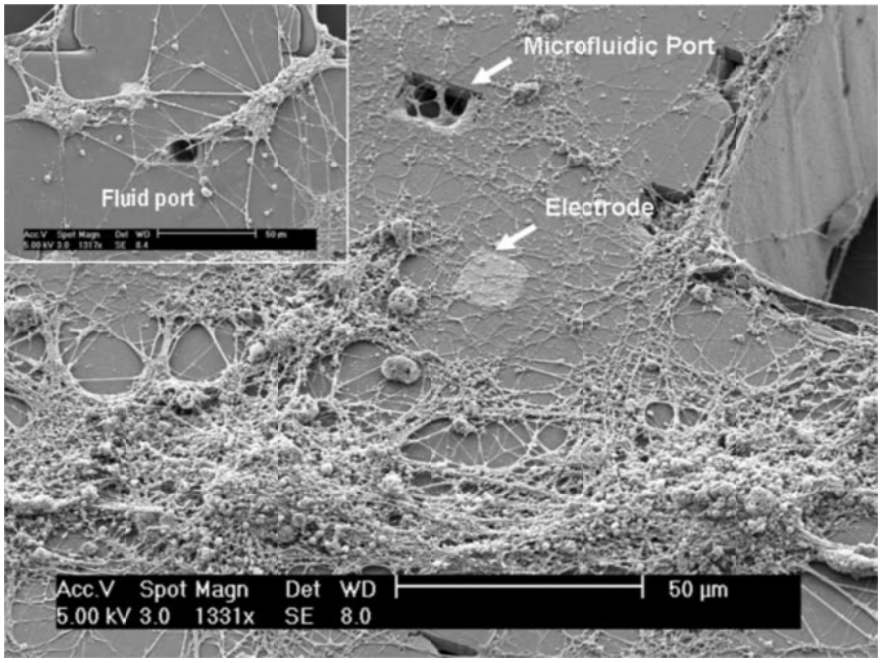

Figure 1: Microscaffold fabricated using MEMs techniques and used for hippocampal neurons. A. SEM micrograph of SU-8 scaffold used to grow E18 rat hippocampal neurons. The holes provide fluid perfusion of the system. B. shows neuronal growth on the scaffold and points out ports and electrodes [16].

Another research group used photolithography to create the base for the hydrogels and then used digital sculpting to create separate extracellular matrix (ECM) areas made of photo polymerizable gelatin methacrylate hydrogels to accommodate three different cell types (neural cells, embryonic stem cells, and human umbilical vein endothelial cells) [17]. UV light was used to crosslink and shape the gels and the study found that if the light was used for 30 sec or less, cell viability was not grossly affected by damage from the UV light, figure 3 [17]. The method of laying down separate layers of ECM and cells effectively separated the cell types. The research done thus far on brain bioreactors demonstrates that hydrogels can be used to make a more complex neuronal cell culture that can be stimulated by microarrays.

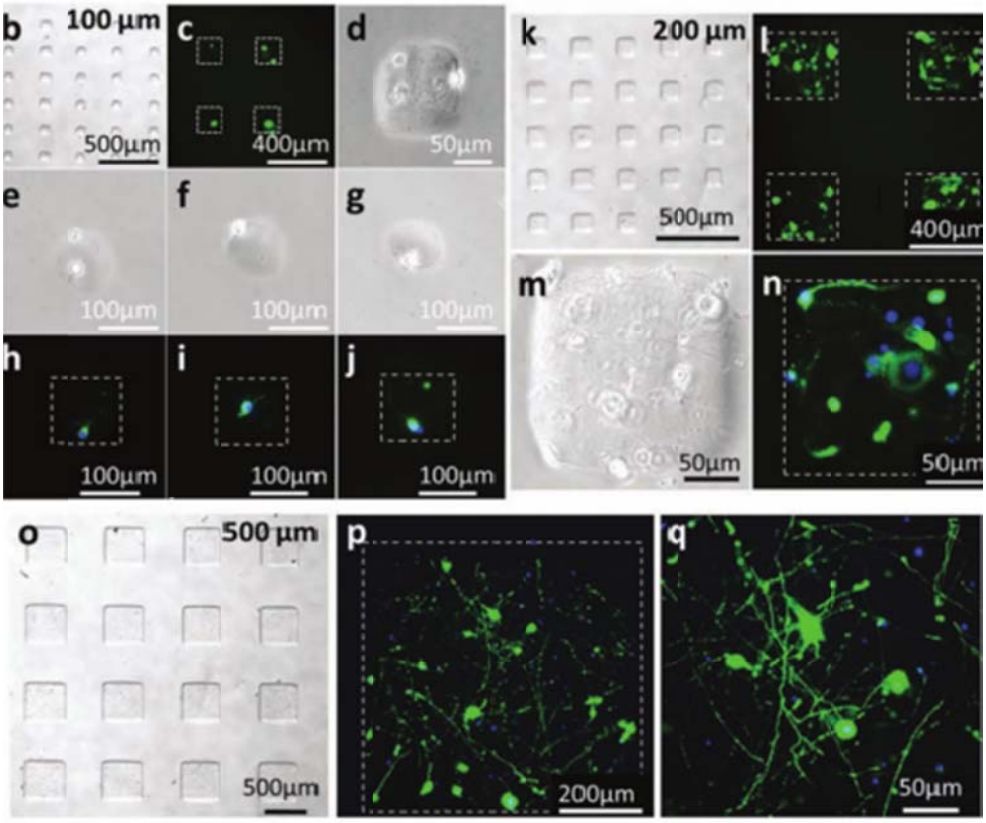

Figure 2: Digitally sculpted hydrogels to support neuronal growth. Figure 3 Illustrates the use of hydrogels with ECM components to stimulate neuron growth. B-j neurons on digitally sculpted 100 μm elements, k-n in 200 μm elements, o-q in 500 μm elements. The green staining is anti-tau and the blue is DAPI [17].

Finally, a study published in PNAS in 2014 perhaps represents the most advanced work in neural tissue engineering. This study by Tang-Schomer et al used a silk protein based scaffold with collagen, assembled as six concentric circles, with each section seeded separately with neurons prior to assembly and the center fashioned from collagen gel matrix [18]. The result was neuronal structures that resembled the cortical tissue, specifically the multiple lamina of the cortex with cell bodies (grey matter) focused in the concentric rings and axons in the center (white matter), figure 4 [1, 18]. In addition to creating a scaffold that more closely resembled architecture in the brain than most designs, the scaffold supported densely seeded cells, with approximately 8,000 cells/mm^3 and supported the cells for up to nine weeks [18].

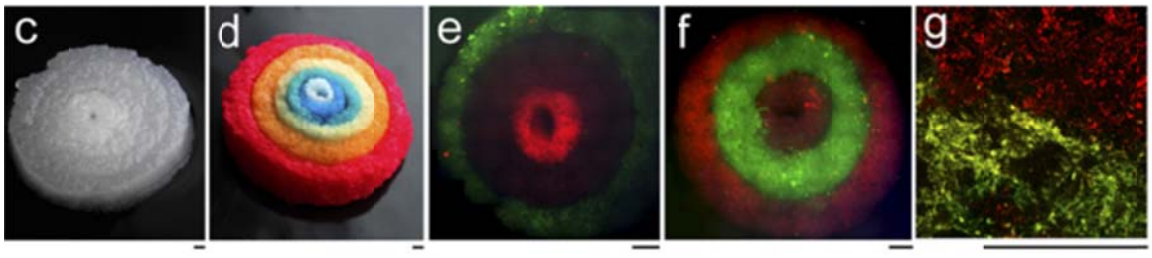

Figure 3: Modular design of concentric circles made from silk scaffold and seeded with rat primary cortical neurons. The concentric circles are made from silk scaffold and collagen and seeded with rat primary cortical neurons. C shows the scaffold in natural colors, d shows the scaffold with dyed rings, e-g show staining of the rings with different live stains for neurons, [1,1'-dioctadecyl-3,3,3',3'-tetra-methylindo-carbocyanine

perchlorate] (red) and [3,3'-dioctadecyloxa-carbocyanine perchlorate] (green). Scale bar is 1mm [18].

Neural tissue scaffolds incorporate technology from various disciplines to create the most effective design to support neuronal growth and have vastly improved over the last ten years. The design that is evaluated in the following pages investigates a fractal design created through the use of MEMs fabrication techniques because the design can be specifically controlled.

This research conducted in these experiments specifically addressed which fractal based scaffold is best suited for neuronal cell culture. The fractal based scaffolds were created using MEMs fabrication techniques, which is the same technology used to create microchips. MEMs fabrication can be done using a variety of material selected based on properties such as biocompatibility, linear aspect ratio, and electrical conductivity. MEMs fabrication begins with a computer assisted drawing (CAD) file, so the scaffold dimensions are highly controllable. This research specifically focused on evaluating which existing fractal pattern was best suited to neuronal growth, figure 2.

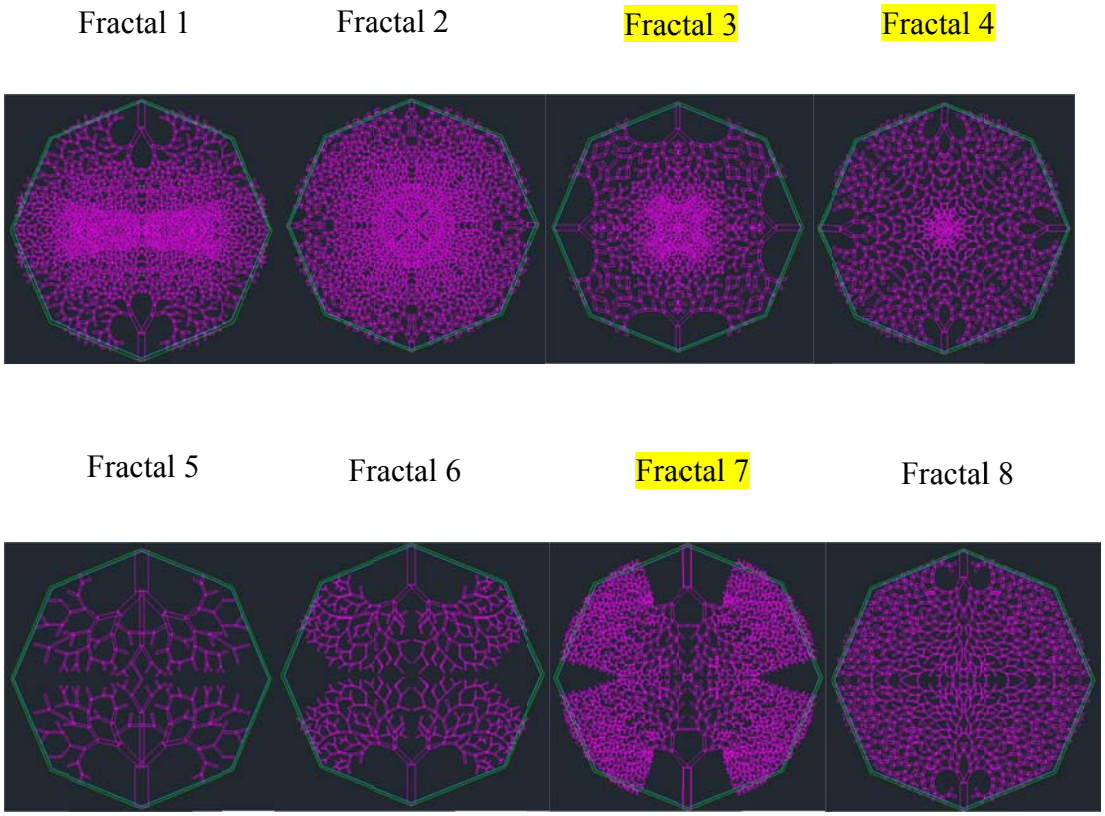

Figure 4: AutoCAD drawing of the nine original fractal designs. The fractal titles highlighted in yellow (designs 3, 4, 7, and 9) were selected for neuronal cell culture. The results from the experiment found that there was a difference in neuronal growth between F9 and F4 and F9 and F7, in both cases F9 had less growth. See results for more details.

To address this question, the following specific aims were developed:

1. Assess the biocompatibility of TiO2.
2. Assess the free standing scaffold created with micro-electro mechanical fabrication for neuronal growth.
3. Assess the ability of neurons to follow complex fractal patterns. For this aim the following hypothesis was formed:

   Null hypothesis: There is no difference in the quantity of neurons, total dendrites on neurons (annotated from here on as dendrites (neurons)), neuronal clumps (referred to as clumps from here forward), and total dendrites on clumps (annotated from here on as dendrites (clumps)) between four different fractal scaffolds.

   Alternative hypothesis: There is a difference in quantity of neurons, dendrites (neurons), clumps, and dendrites (clumps) between four different fractal scaffolds.

For the experiment, the independent variable (IV) was the fractal type and the dependent variables were number of neurons, dendrites (neuron), clumps, and dendrites (clumps).

The experiment described in the subsequent pages addresses this hypothesis and also addresses biocompatibility for neurons, neuronal placement, long term growth (days in vitro 11), and 3D growth. The results of the research described within this thesis provide invaluable insight for the design and development of the next generation of the

bioreactor. Developing a brain bioreactor will provide a platform on which researchers can address complex questions regarding the central nervous system (CNS).

Chapter 2 MEMS FABRICATED FRACTAL SCAFFOLDS

2.1 – Fractal Scaffold Design

The scaffolds used in this experiment were initially designed for a breast cancer model in the Smart Sensors and Integrated Microsystems (SSIM) lab and those procedures are outlined in "Development of Fractal and Electrode Components for Organotypic Culture in a Novel Three-Dimensional Bioreactor System", the reference for which is at the end of this work [19]. There were nine fractal designs created using AutoCAD software, figure 1. The designs were drawn using bifurcations, choosing the angle for each design at random. The fractals vary in their pattern density and each fractal array has an outer diameter of 1 cm. In CAD, a line tool was used to create the fractal pattern and then gave a width to the line, versus using the rectangle tool in which width is a native property. This is an important distinction because it identifies one of the limitations of the design process. The width given to the lines is not an "actual" width when interpreted by CAD and therefore cannot be used to determine the surface area of the fractal. Although there were methods that could be used outside of CAD to calculate the surface area, they were not pursued for this experiment. Consequently, the number of neurons per mm^2 in this design iteration was not calculated. Instead, the fractals can be evaluated qualitatively by looking at the surface and comparing different fractals. The second limitation identified in the fractal design is that they were drawn "free hand" versus using an algorithm. Using free hand to design the fractals gave the creator freedom to truncate the fractal as necessary to avoid overlapping with another area of the fractal and it also resulted in very intricate fractal designs. However, the hand drawn

pattern cannot be replicated to include future parts of the bioreactor such as media ports or channels. The use of the line tool to draw the fractals also limits the CAD tools available to replicate the drawings because a line does not have the same properties as two-dimensional shapes which are needed to more easily replicate the design. Despite the limitations of the fractal design in regards to future generations of the bioreactor, they are well suited to address how the neurons grow on different densities of fractal patterns.

2.2 – Fractal Scaffold Selection

There were nine original fractal designs and four were selected to be tested for neuronal growth, figure 1. The fractals chosen to be tested were fractals 3, 4, 7, and 9, highlighted in figure 1. Fractals 5 and 6 are the least dense fractals and these were eliminated because they broke frequently when handled. Fractals 3, 4, and 7 were chosen because they contain areas of both very dense areas and less dense areas. These fractals resisted cracking even when moved multiple times throughout the experiment. Fractal 9 was chosen because it is the densest of the fractals. Fractal 9 had the tendency to crack along the center when it was picked up from a wet surface because it does not have any convenient areas to grab with the forceps and its dense pattern increased the surface tension which made it difficult to pick up in confined areas (24 well plate) without cracking. In open areas, such as the 6" wafer, it was not as much of a problem because a scalpel could be slid underneath providing an edge to grab with the forceps. A future design consideration should be to include an area large enough to be picked up with forceps in order to minimize scaffold cracking.

Chapter 3 – PREPARING THE FRACTAL FOR NEURONAL GROWTH

3.1 – Neuron Growth

Although neurons are only one of several cell types in the CNS, they are considered the most important cell type because their health and connectivity is central to CNS health. They are also amitotic (with limited exceptions) which makes injury or illness to the CNS nervous difficult to treat. Neurons arise from epithelial cells and are initially motile during cellular migration [20]. Figure 5 depicts the two step process of rodent neurogenesis; epithelial cells give rise to radial glia cells which make intermediate progenitor (IP) cells which divide once to produce two neurons [20]. Figure 6 illustrates a neuron in which the neuron develops a cytoskeleton to move into position and then sheds the microtubules [20]. The use of filaments allows the neurons to move and it is important to consider the limited motility that neurons possess when creating a bioreactor in which the placement of neurons is important [20].

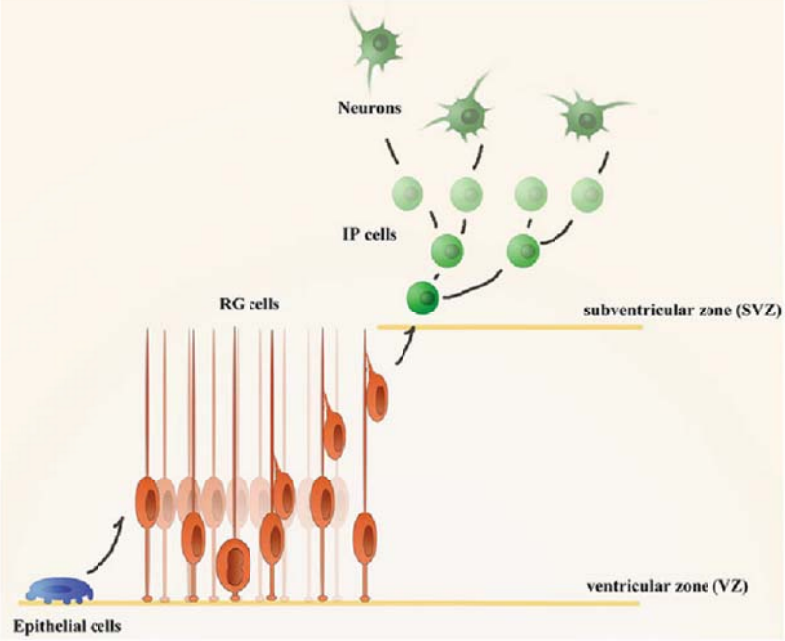

Figure 5: The two step process of rodent neurogenesis. The two step process of rodent neurogenesis, epithelial cells give rise to radial glia cells which make intermediate progenitor (IP) cells which divide once to produce two neurons [20].

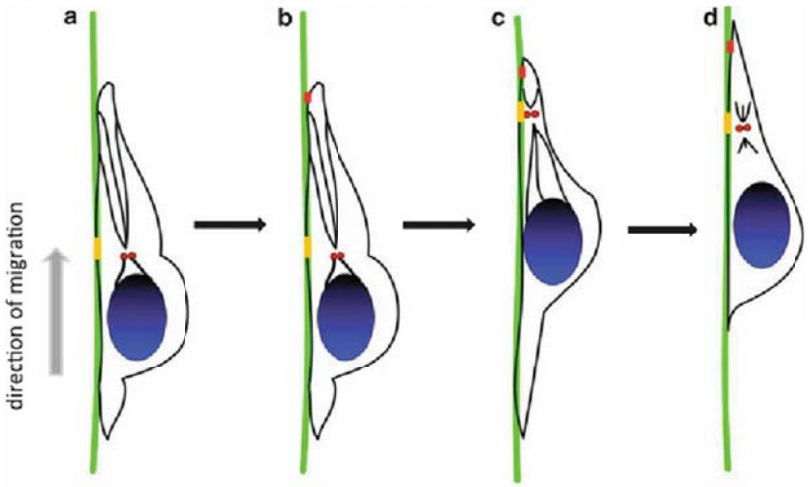

Figure 6: The process of neuronal migration. Illustration of a neuron in which the neuron develops a cytoskeleton (a) to move into position on the substrate (b) and then creates microtubules and nuclear translocation (c) before reshaping the trailing edge (d) [20]. The cytoskeleton responds to the ECM to move into position. During this movement, rodent neurons may move a few hundred microns where human neurons may move up to 2 cm [20].

Once a neuron is in position the axons and dendrites continue to respond to ECM signals to create the complex neural environment. The dendrites bring electrical signals in to the cell body while axons take electrical signals away from the cell body. Dendrites and axons connect to create the billions of synapses within the brain. Dendrites have filopodia which extend toward the axon growth cone [21]. In addition, dendritic shafts contain microtubules that assist in dendrite health [22]. Axons also develop filopodia as well as lamellipodia from the growth cone which respond to the ECM to form connections [23]. In order for a neuronal bioreactor to be effective, it needs to provide a healthy ECM for neurons in order to encourage axon and dendrite outgrowth which will form complex synapses.

3.2 – Neuron Surface

Neuron outgrowth is dependent on a healthy cytoskeleton where axons and dendrites can create synapses with axons and dendrites from other neurons. The microfilaments, intermediate filaments, and microtubules of the cytoskeleton help form the complicated morphology of neurons [24]. The interaction between the cytoskeleton and the ECM is also critical to neuron survival [24]. The cytoskeleton must be anchored to the substrate in order for the motor protein, myosin, to assist in movement of the growth cone [24]. When the cytoskeleton is not anchored to the substrate 'treadmilling' occurs when the actin microfilaments move rearward [24]. There are many proteins that play a role in the neuron cytoskeleton; one category, the immunoglobulin superfamily, includes the neural cell adhesion molecules (NCAM) which assists in cell surface adhesion to substrates [25].

3.3 – Cell Adhesion-mediating (CAM) Protein

The NCAM proteins possess anionic binding sites and therefore need a cationic binding site. In neuronal cell culture this is often made possible through the use of cell adhesion-mediated proteins. This experiment made use of poly-L-lysine (PLL) coated substrate to improve cell adhesion with NCAM ligands on the neuron surface. PLL is the digestible form of poly-D-lysine (PDL) which is frequently used with stiff substrates as was used in this experiment [26]. PLL was used in this experiment due to a greater than 6 week waiting period for PDL from Sigma Aldrich. PLL is not an uncommon choice of adhesion for substrates and is recommended in a Nature Protocol for culturing hippocampal neurons for up to four weeks [27]. Because of this, PLL was seen as an acceptable substitute for PDL.

PDL plays the role of a cell adhesion-mediating protein. PDL is a synthetic class of polyamines which are polycations, meaning they have multiple amino acids and multiple cation sites. PDL binds strongly to negatively charged surfaces and still has cationic surfaces available for cell adhesion sites [28, 29]. Since PDL is synthetic, it is immune to digestion from the cell and will not be involved in cell signaling.

PDL must adhere to the substrate in a manner that will allow the opposite cationic side absorb to the ligands on the neuron surface. The selected substrate must have a slightly hydrophilic surface with a contact angle of approximately 50°. If the substrate is too hydrophobic (contact angle greater than 100°) then the cell adhesion-mediating (CAM) protein binds in a denatured form and do not provide that appropriate ligand for the cell adhesion receptors, see figure 7 [30]

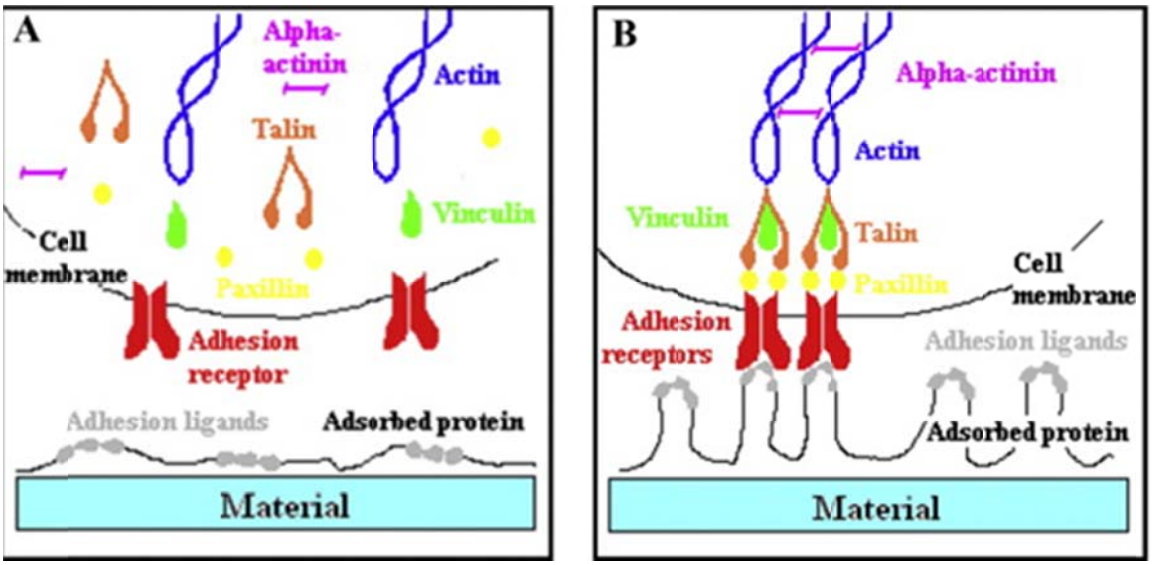

Figure 7: Effect of hydrophobic and hydrophilic material on CAM proteins and cell adhesion.

A. Cell adhesion mediator absorbed onto a hydrophobic material denatures and will not attach to adhesion receptors on cell.
B. Cell adhesion mediator absorbed onto a hydrophilic material maintains its shape and will attach to adhesion receptors on cells. [30]

Highly hydrophilic substrates also negatively affect cell attachment, particularly for longer cell cultures [30]. Highly hydrophilic substrates (contact angle less than 35°) bind weakly or not at all to the CAM protein, so there is little or no binding to the cell's adhesion receptors [30]. PDL met the criteria to be an effective CAM protein for neuronal growth, however it is most likely not the best choice for a CAM when working with titanium coating, which will be discussed later.

3.4 - Substrate Selection

3.4.1 – SU8

As discussed in 3.2, a substrate for neuronal growth must be able to bind to the CAM; in addition, the selected substrate must also be biocompatible. The fractals were fabricated using SU8 polymer which is an epoxy based negative photoresist, made of Bisphenol A Novolac epoxy, and is very hydrophobic, with a contact angle of 78°, consequently the PDL would be expected to denature as it attaches to the SU8 and thus not be an effective CAM protein for the neurons [31]. SU8 can be rendered hydrophilic through the use of oxygen plasma treatment or ethanolamine which would improve its adhesiveness [32, 33].

Although the SU8 surface can be modified to increase its adhesiveness, it is not biocompatibile with neurons. In a study done on compatibility of SU8 (2000) with E17 or E18 rat embryonic cortical and hippocampus neurons, it was found that even neurons plated adjacent to the SU8 (2000) were not viable [34]. X-ray photoelectron spectroscopy analysis of the SU8 (2000) indicated that fluorine and antimony were the most likely toxic substances leaching from the SU8 (2000) and causing cell death [34].

The group used various treatments or coatings on the SU8 (2000) and found that three day hard baking, isopropanol sonification, oxygen plasma treatment, or parylene coating improved SU8 (2000) compatibility [34].

3.4.2 – Titanium Oxide (TiO_2)

This experiment used titanium dioxide to coat toxic SU8 (100) fractals and render the fractal biocompatible with the neurons. Titanium dioxide (TiO_2) is used in many medical devices due to its biocompatibility. The oxide layer that forms immediately when titanium is exposed to air, inhibits the inflammatory response of the immune system by breaking down reactive oxygen species at physiological pH [35]. There are very few studies that have been conducted on the biocompatibility of TiO_2 and neurons. In the only research study found specifically investigating the interaction between TiO_2 and neurons, researchers used rutile disks coated in poly-l-lysine (PLL) and reported that there was good neuronal growth up to 10 days in vitro (DIV) of cerebral cortex neurons from E14 Wistar rats [35]. Although they did note that DIV4 had about twice as many viable neurons as DIV10. The researchers suggested that the reduction in neurons could possibly be attributed to inconsistencies in the PLL coverage. In this same study the rutile disks had rough topographical features due to the pebble like appearance of the disks and researches reported that at times the neurite outgrowths followed the path in the disks and at other times they did not [35]. Additionally, a study conducted on the compatibility between spiral ganglia and titanium discs (coated in PLL and laminin) demonstrated that the titanium disks supported the spiral ganglion as well as or better than the plastic control, also coated with PLL and laminin [36]. Based on the available

research, TiO2 was a good choice as a fractal coating, and the lack of research on the interaction between titanium and neurons highlights an area that needs further research.

Chapter 4 – MATERIALS AND METHODS

4.1 - Fabrication of Fractal Scaffolds

The fractal scaffolds were fabricated using photolithography by two previous students in SSIM and the process was refined with Dr. Auner's guidance and will be briefly outlined below and can be found in greater detail in the references [19]. SU8 is a negative photoresist that can be applied in relatively thick layers, greater than 200 μm, with a high aspect ratio that results in nearly vertical side walls [37]. The general flow when using SU8 is to pretreat the substrate, coat with SU8, soft bake, expose, post expose bake, develop, rinse and dry, and hard bake [19]. This development process resulted in fractal scaffolds with 100 μm thick walls and a high aspect ratio. The relative thickness of the walls created scaffolds that were sturdy enough to be lifted off the wafer and be used as free standing scaffolds.

As part of this thesis work I conducted the liftoff of the SU8 from the SiO_2 wafer and collaborated with members of the lab to have them coated with TiO_2. Liftoff of the scaffolds was performed using hydrofluoric (HF) acid in a 5:1 buffer. First the wafer was diced to increases contact areas for the acid. Next the fractals were placed in a HF solution in an ultrasound bath for approximately 90 minutes. Once the fractals had lifted off the surface of the wafer, they were rinsed for five minutes with deionized water and then left to dry in the clean room.

To help prevent neuron toxicity from the SU8 (100), the fractals were hard baked at 150° C for 72 hours and coated in TiO_2 using sputter deposition. The fractals were coated using a KDF Ci load lock sputter deposition system powered by DC plasma (DC

Pinnacle Plus by Advanced Energy) that used a 6" titanium target. The chamber was pumped down with a cryo-pump to $1x10^{-8}$ Torr. The target was cleaned for two minutes with plasma created from argon gas and then 16.67 minutes of deposition on the wafer at 75 W to give a 1000 Å titanium coating. The thickness was confirmed using a Dektak profilometer to analyze the depth. The fractals were coated on one side and then removed and coated on the second side to limit SU8 (100) toxicity to the neurons.

4.2 – Substrate Preparation

The TiO_2 fractal scaffolds were sterilized via UV light exposure for 15 minutes per side. Then the fractal scaffolds were coated with 100 μg/ml of PLL (Sigma Aldrich, 0.01%, MOL WT 70,000-150,000, P4707, Batch RNBD5244). As a control for the experiment, one well of the 24 well tissue plate (Corning, 3524) was coated with 50 μg/ml of PLL, diluted with sterile distilled water. Both the fractals and controls were left in PLL overnight, but did not exceed 20 hours of coating. The PLL was then removed and the wells and fractals were rinsed once with sterile distilled water. The control and fractals were completely air dried before proceeding. The control wells dried in approximately 15 minutes, while the fractals took between 1.5 and 2.0 hours. The fractals were then moved to 24 well plates that had not been coated with PLL to try and minimize interference from neurons growing on the bottom of the well.

The fractals were coated with a greater concentration of PLL than the 24 well plates because initial optimization experiments, the higher concentration of PLL yielded greater neuronal growth on the fractals but did not encourage greater growth in the controls. In experiments 1, 2, and 3 the PLL coated surfaces were used immediately for

cell culture. In experiments 4 and 5 the plates were prepared 24 hours prior to the arrival of the neuronal cells and wrapped in paraffin film and stored at 4° C. According to Life Technologies protocol, it is acceptable to store PDL coated surfaces for up to one week in this manner [38]. The plates were allowed to come to room temperature before cell plating.

Initial experiments revealed that the fractals were prone to floating in the well, which posed the possibility that the neurons would be exposed to air during the experiment. To prevent this from happening, 10 μl of 2% agarose mixed in PBS (heated at 100° C to liquefy and sterilize) was placed in the well at the 12 o'clock position and the fractal was immediately placed on top of the liquid. The gel was mixed with PBS to maintain a neutral Ph and 2% was chosen to deter neurons from growing in the gel [39]. The fractals were placed such that only part of the fractal contacted the agarose. The agarose gelled before cells were introduced to the wells. Although through the course of the experiment the gel broke free from the bottom in some wells, the fractal remained submerged in the media and the neurons were not exposed to air. In some instances there was growth on top of the agarose, but due to the translucence of the agarose it was difficult to determine if the neurons grew into the agarose. In addition, the amount of agarose covered such a small area compared to the fractal, that it was not considered an interference with the experiment.

4.3 – Neuronal Cell Culture

4.3.1 – Initial experiments

The initial experiments to determine optimal PDL coverage used dissociated rat cortical neurons from E18 Fisher 344 rats (Life Technologies) cryopreserved in DMSO. The initial cell count, made using a hemocytometer, contained the guaranteed amount of viable cells, however successfully culturing the cells was highly dependent on the B27 (media additive) lot number, and PDL lot number. Consequently there was very little neuronal growth despite strictly adhering to the provided protocol. Because of the poor viability of the cryopreserved cells, fresh cells purchased from BrainBits LLC were used for the primary experiments. The neurons from BrainBits were dissociated cortex neurons from E18 Sprague Dawley rats, delivered overnight. The optimal PDL coverage for the fractals with the cryopreserved Life Technologies neurons was 100 μg/ml. This coverage was within the acceptable range of the BrainBits protocol, so further optimization experiments were not conducted with the change in neurons [40].

However, an initial experiment was conducted with the BrainBits neurons to determine the ideal number of neurons to plate on the control and fractal. Control wells and fractals were plated in triplicate with the following number of cells: 16,000 cells (recommended protocol), 50,000 cells, and 100,000 cells (recommended number not to exceed). At the end of 11 DIV, the different cells densities did not have much effect on the growth in the control wells. In contrast, the fractal wells had no neuronal growth in the 16,000 cell wells and very little growth in the 100,000 cell wells but good growth in the 50,000 cell wells, so all experiments were plated at 50,000 cells (controls and fractals).

4.3.2 – Neuronal Cell Plating

The experiment was conducted five times, in triplicate. The five experiments came from three different lot numbers supplied by BrainBits. The BrainBits protocol was followed with the above outlined changes in cell density and the use of PLL instead of PDL as well as the increase in PLL concentration used to cover the fractals. In addition, the protocol called for aggressively triturating the neurons no more than five times to break up the cloud of DNA and cellular material present in the neurons when they arrived [40]. Triturating five times was not enough to break up the cloud, so triturating was continued until the cloud was broken up more thoroughly. At most, the cells were triturated was fifteen times, which did not affect cell viability, although there was still a small cloud present in the media. In the future, these cells could potentially be triturated further without concern over cell death to achieve better separated cells. There was some clumping noted when the cells were first plated, which is not ideal because the neurons will not separate from each other to form synapses, however, there were many areas of adequately separated cells that could form synapses.

The cells were counted using trypan blue and the hemocytometer cell counting method. The cells were mixed with trypan blue in a 5:1 ratio and then 10 µl was placed on the hemocytometer and looked at through the light microscope. The cells were counted as live if the trypan blue did not cross the cell wall. Next the total cell count was estimated based on the live cells counted, volume of the hemocytometer, and the ratio of cells to trypan blue. After the cell count, the wells were plated with 50,000 cells per well. Approximately 25 µl of media contained 50,000 cells in each experiment. The cells were pipetted into the center of the fractal, avoiding the area with agarose, although in some

instances the agarose had spread out underneath the majority of the fractal and could not be avoided. The cell plates were placed in the incubator (37° C, 5% CO_2) and allowed to settle for about 15 minutes before adding 500 µl of neurobasal media supplemented with 2% B27 additive and .25% glutamax [38]. The goal behind plating the cells with a minimum amount of media was to plate as many cells as possible onto the fractal. Letting them settle for 15 minutes allowed time for cell attachment to the fractal before adding additional media. Allowing longer time to settle was inadvisable because the small amount of media with the cells started to dry out, risking cell death. After 500 µl of media was added, the cells were returned to the incubator and fed every 3-4 DIV by replacing 250 µl of media with 250 µl fresh media. The cells were cultured for 11 DIV and then immunohistochemistry (IHC) was performed on the wells with fractals so that they could be photographed using an Xcite 120 mercury bulb.

4.4 Immunohistochemistry (IHC)

The Life Technologies protocol for IHC of neuronal cells was used in order to visualize the neurons on the fractals [38]. The control wells served to monitor the health of the neurons over the cell culture period and were not used to compare with the fractals for neuronal growth and were therefor not stained. After fixing the cells with paraformaldehyde, the neurons were stained with primary antibody, mouse anti-MAP2 diluted in 5% goat serum and incubated overnight at 4° C. Mouse anti-MAP2 attaches to MAP2 which is found in the cell bodies and dendrites of neurons. Not long after axons and dendrites are formed, tau segregates into axons while MAP2 segregates into dendrites [41]. Therefore, axons are not visible when staining MAP2, however, the

amount and appearance of dendrites provided ample information about the neuron's health. If axons are required to be visible, then the tau present in axons can be tagged and stained, which was not done in this experiment. After overnight incubation with the primary antibody, the cells were stained with secondary antibody, Alexa Fluor 488 goat-anti mouse diluted in 5% goat serum and left at room temperature for 60 minutes. The cell plates were covered with aluminum foil to help protect the Fluor from light. At the end of 60 minutes, the excess dye was rinsed away and ProLong Gold antifade reagent was added to each fractal. The fractals were removed from the 24 well plate and placed top side down on glass slides with a coverslip on top. This was done so that both sides of the fractal could be observed with the microscope.

4.5 Imaging

The neurons were imaged using a Nikon TE-2000-E inverted light microscope and attached X-Cite-120 Q for fluorescence illumination. The control wells were imaged using 10x light microscopy and each well was photographed five times, with the exception of the first experiment, which captured one image for each well. Each fractal was imaged five times using 10x magnification, the X-Cite 120 Q laser, and the blue filter on the microscope. A perfect data set would have provided a total of 75 images for each fractal. However, in experiment 5, there was no replicate 3 for fractal 4 because it had broken into small pieces and there was not a replacement available. Consequently, fractal 4 had 70 out of 75 images.

The fractal images were taken with the following procedure. The fractal was focused on at the 12 o'clock position and then surveyed in a counter clockwise manner

for an area of neuronal growth. Once an area of neuronal growth was found, an image was taken, then the stage was moved to the adjacent area where another image was taken and this was repeated until five images were captured. Next, the remaining area of the fractal was surveyed for areas that had better growth than the areas previously imaged. If a better area was found, then the area was imaged to be used as a replacement image for one initially taken. The images used in analysis represent the best areas of neuron growth on the fractal.

Next the images were loaded into Image J, the open source image analysis program available from the NIH. The Image J counter was used to count neurons, dendrites on neurons, clumps, and dendrites on clumps. Originally only neurons and neurons on dendrites were counted; however because there was a noted problem with clumping I felt it was important to test if certain fractal patterns were more likely to clump (they are not, see results for more information).

CHAPTER 5 – ANALYSIS

5.1 – Qualitative Analysis

1. The cells were very robust. The cells grew on the bottom of the wells that had fractals, but no PLL and continued to grow for the 11 DIV. There was no neuronal growth expected on the bottom of the wells with no PLL, figure 8.

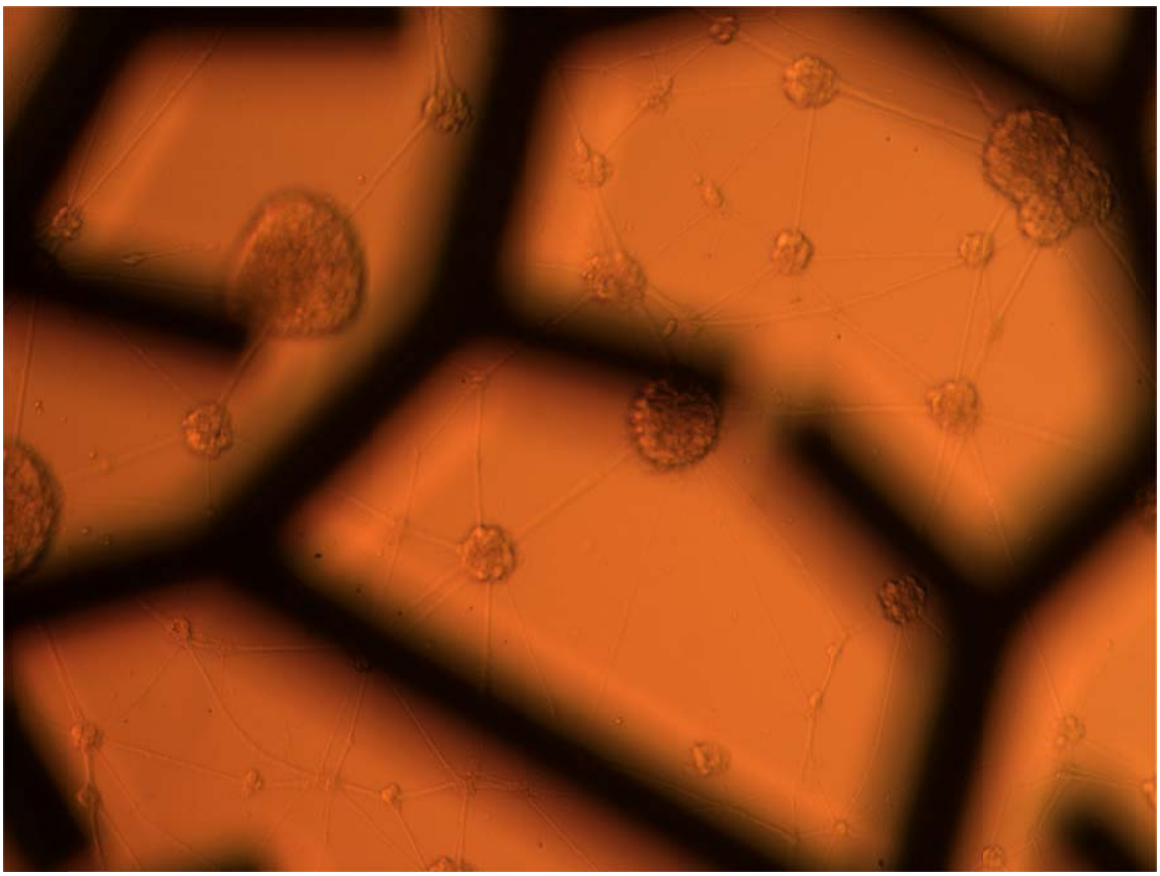

Figure 8: Experiment 1, DIV 11 picture at 10x of F4. This photograph shows healthy neurons growing on the bottom of a well with no PLL. The result was unexpected since PLL is considered necessary to facilitate attachment between the cells and the plate.

2. The cells were difficult to break up completely. Future work using these cells could try to triturate more often to try and more thoroughly break up the cells. Clumping cells also affects cell count, however, there were no cell clumps on the hemocytometer in any of the cell counts. Although clumping was a problem with the experiment, there were many cells that dissociated completely and had an opportunity to form synapses with nearby cells. See figures 9 and 10 for a comparison of clumping and non-clumping cells.

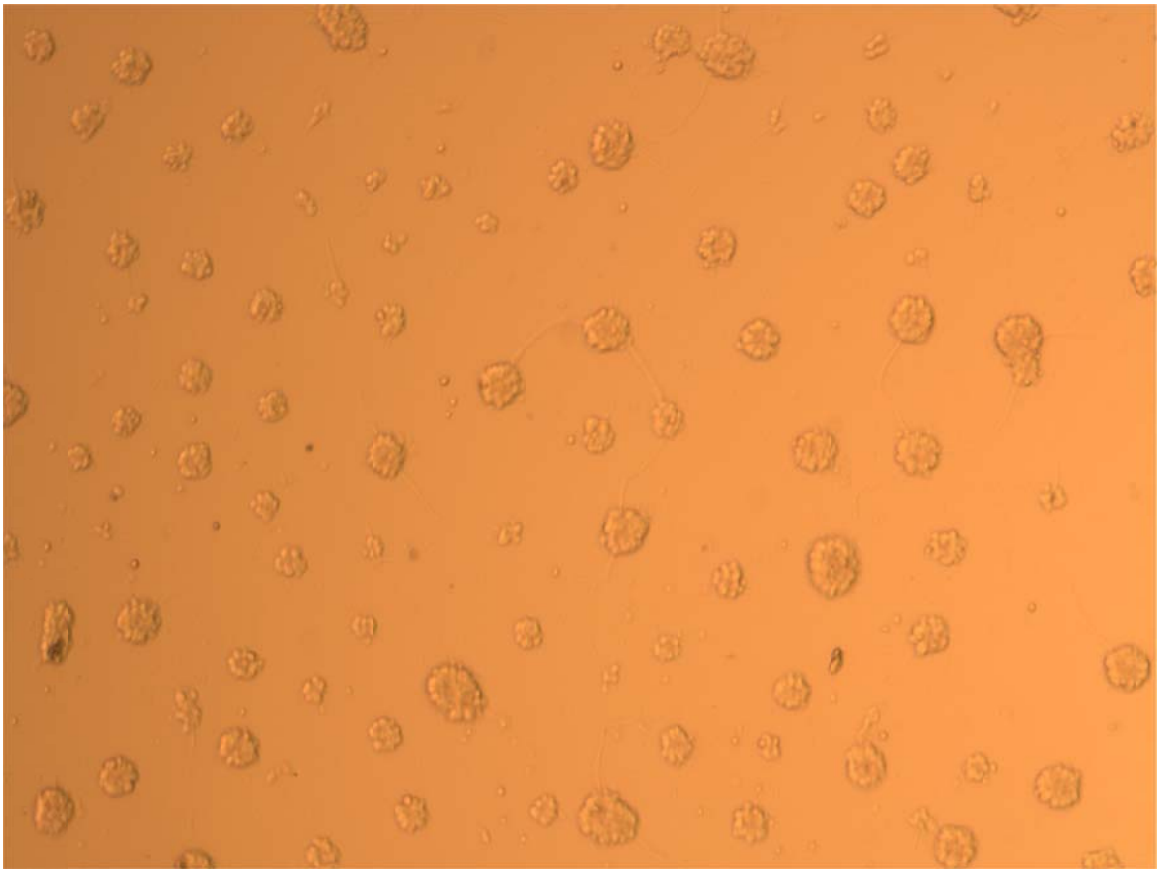

Figure 9: Optimization of cell volume, 16,000 cells, 3 DIV at 10x. This image is from the experiment done to determine the best cell volume for the experiment. These cells are plated at 16,000 cells/well. This demonstrates the clumping that occurred with the cells, despite triturating more than the protocol recommended.

Figure 10: Optimization of cell volume, 50,000 cells, 3 DIV at 10x . This picture is from the experiment done to determine the best cell volume for the experiment. These cells are plated at 50,000 cells/well. Although some cells came out as clumps, there were other times that the cells were separated as single cells.

3. Over the course of the experiment, the cells that started out as single cells started to clump. According to BrainBits' protocol, after 4 DIV axons and dendrites start to grow and at 7 DIV, synapses begin [40]. This was observed in the control wells during the experiment, however after 7 DIV the cells began to clump and there was a severe reduction in synapses. See figures 11 and 12 for comparison. This observation is different from the observation that cells came out as clumps at the initial cell plating. Even cells that initially plated as single cells started clumping after 7 DIV. This was

identified as one of the key limitations of the controls and scaffolds and will be examined in “Discussion”.

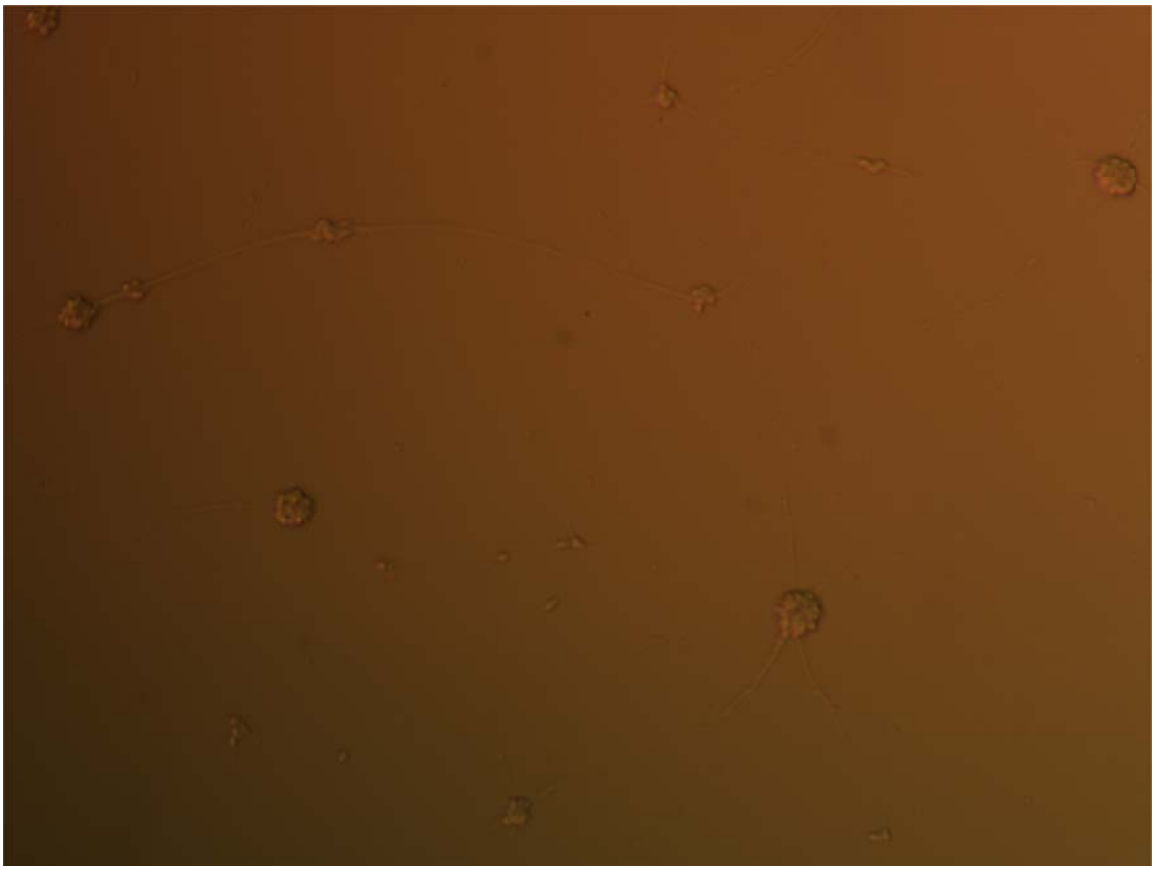

50 µm

Figure 11: Experiment 2, Control well 1, 6 DIV, 10x. Although there is clumping in this well, the neurons are developing synapses.

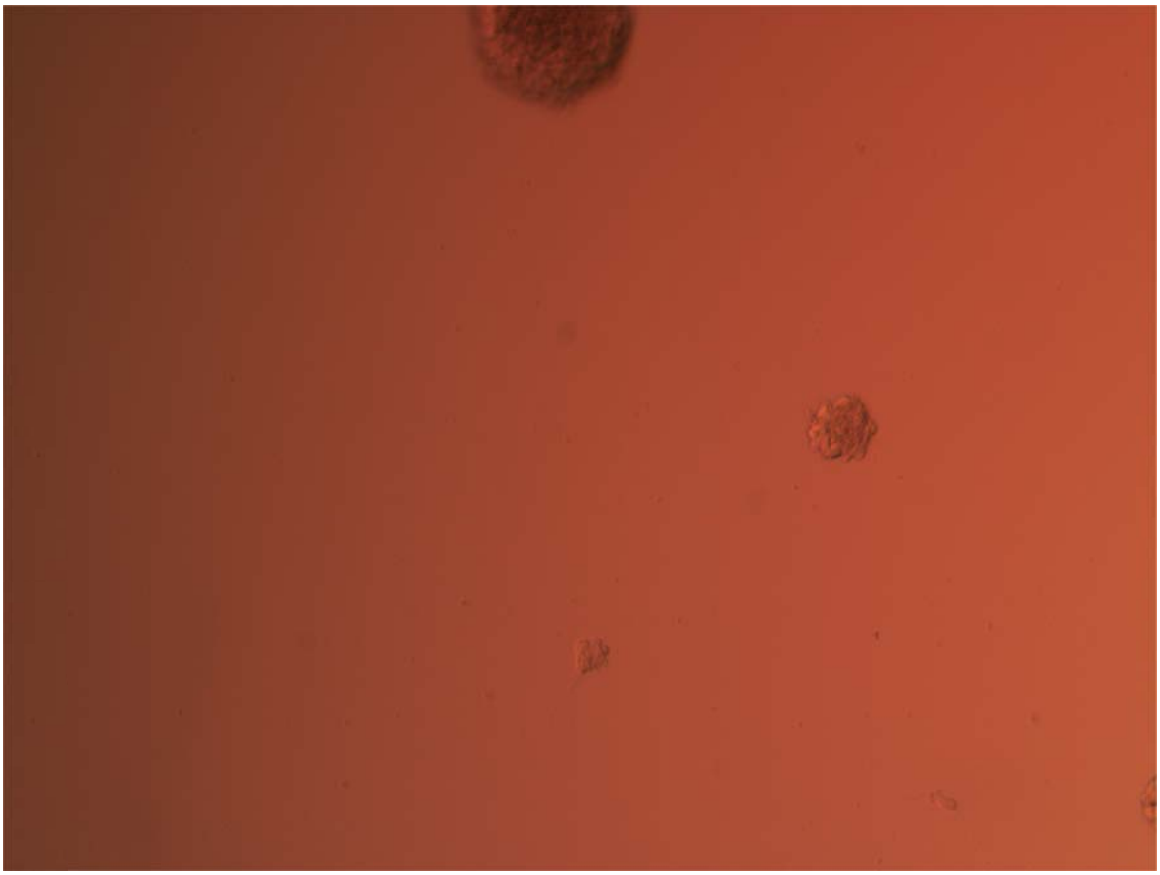

50 µm

Figure 12: Experiment 2, Control well 1, 11 DIV, 10x. This picture is taken of the same well as Figure 11. There are virtually no synapses or single cells. This was indicative of all controls; synapses peaked around 7 DIV and then decreased.

4. The neurons grew on all surfaces of the fractal; bottom, sides, and top. There were also synapses between the neurons located on different parts of the fractal as well as synapses between neurons on the bottom of the well and the fractal. The fractal scaffold did provide for 3D growth of the neurons, see figure 13. Figure 13 exhibits healthy neurons that appear as plump ovals with multiple synapses connecting to neighboring neurons. Many of the neurons were contained in the interior structures of the fractal branches and at some points in the images, dendrites appear to cross to other surfaces of

the fractal. There is an out of focus glow in parts of the images which are from neurons growing on the other side of the fractal. Figure 14 captures some of the primary challenges in culturing neurons in this experiment. Figure 14 A show neurons that are alive but appear unhealthy because the cell body lacks a circular and plump appearance. Also there are short dendrites present, but there are few if any synapses with neighboring neurons. Figure 14 B exhibits neuronal clumping which was a problem during the experiment, although the clumps appear healthy; they do not facilitate long term growth of neurons.

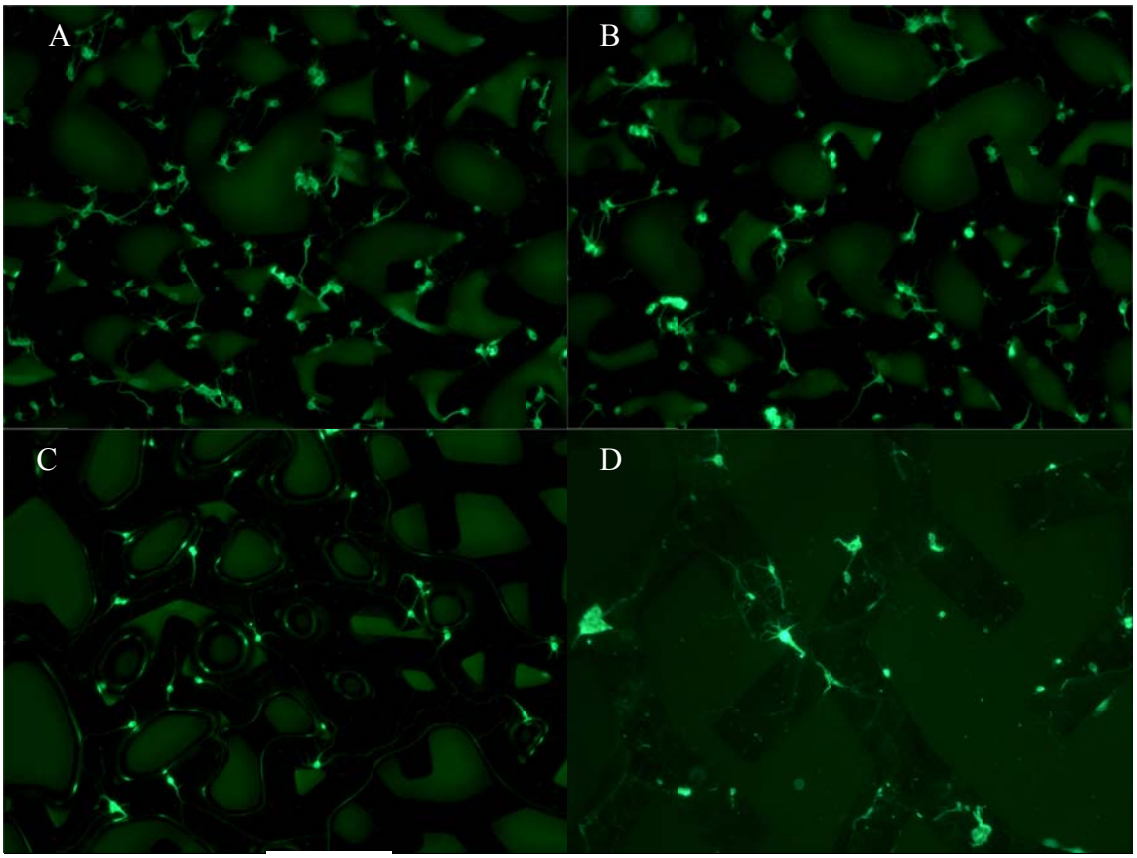

A – C scale: 50 μm

D scale: 50 μm

Figure 13: Examples of healthy neuronal growth on fractals after 11 DIV. A-C. Experiment 5, F9 backside, 10x contained many healthy neurons with multiple synapses. There is a noticeable glow from beneath the fractal that are from neurons on the other side. Dendrites can be seen following the fractal path. D. Experiment 3, F4, 20x is an example of healthy neurons, with one in the center extending a dendrite across a gap.

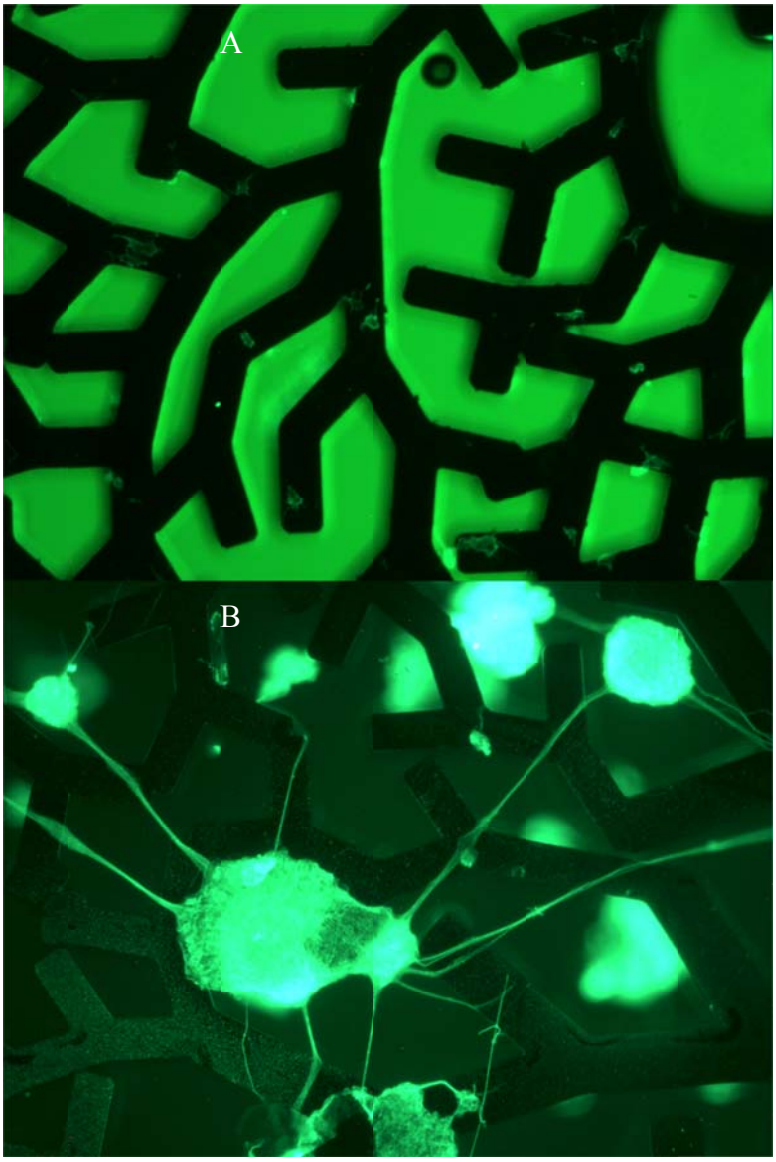

Figure 14: Examples of unhealthy neuronal growth on fractals after 11 DIV. A. Experiment 1, F7, 10x. Neurons that stained well enough to be imaged, but do not appear healthy because the cell body shape lacks symmetry and there are no dendrites extending between neighboring neurons. B. Experiment 2, F7, 10x. The cells were difficult to

break up at times and plated in clumps despite thorough trituration. The dendrites crossed the gaps between fractal branches.

5. Although the neurons were pipetted onto the fractals in small volumes and allowed to set for 15 minutes, many of the neurons washed off the fractal surface immediately, see figure 15. Figure 15 was taken immediately after plating the neurons and it is apparent that the neurons are not contained on the top of the fractal surface. Consequently, when the fractal was imaged after 11 DIV, there were very few areas populated with neurons. An estimated 90% of the fractal surface was absent of neurons. This was considered a major limitation of the fractal scaffold and will be examined further in the "Discussion" chapter.

50 µm

Figure 15: Experiment 2, F3, 0 DIV, 10x. This photograph highlights the problem with plating the neurons on the fractal. This picture was taken within 20 minutes of plating the cells, before adding 500 µl of media. Although the cells were plated in a small volume, 25 µl, and the cells were released directly onto the fractal surface, many of them get washed off the fractal almost immediately.

5.2 – Statistical Analysis

5.2.1 – Data Collection

The data used in the statistical analysis was collected via the image analysis procedure outlined in section 4.5. Figure 16 provides an example of how the 24 well plate was used with the cell plating on the positive control and fractal repeated in triplicate on each plate. This process was completed five times with three different cortical neuron lot numbers. After IHC, there were five pictures taken of each fractal (an exception is noted below) and the data from the images (neurons, dendrites from neurons, clumps, and dendrites from clumps) was input into the statistical model discussed below.

Table 1: Experimental Setup.

Well	Positive Control	Fractal 3	Fractal 4	Fractal 7	Fractal 9
1	50 µl/ml PLL 50k cells	10 µl 2% agarose 100 µl/ml PLL 50k cells	10 µl 2% agarose 100 µl/ml PLL 50k cells	10 µl 2% agarose 100 µl/ml PLL 50k cells	10 µl 2% agarose 100 µl/ml PLL 50k cells
2	""	""	""	""	""
3	""	""	""	""	""

The table above represents the experimental setup for the cell culture in a 24 well plate. Each column was repeated in triplicate as annotated by the "" to indicate "repeated". This entire setup, represented by the 24 well plate was repeated five times.

5.2.1 – Statistical Tests

The statistical tests were used to evaluate the null and alternate hypothesis.

Null hypothesis: There is no difference in the quantity of neurons, total dendrites (neurons), and total dendrites (clumps) between four different fractal scaffolds and the control.

Alternative hypothesis: There is a difference in quantity of neurons, dendrites (neurons), clumps, and dendrites (clumps) between four different fractal scaffolds.

The statistical models used followed the recommendations found in "Using Multivariate Statistics", 5th edition and were performed using SPSS version 22 [42]. The results were considered to be significant if the α value was .05 or less and the power (β) was .80 or higher. The statistical tests did not include the control because the purpose behind the control was to assess the health of the neurons and it had much greater surface area and only a 2D growing surface, consequently there were far more neurons in the control plates than on the fractal. Adding data from the controls would have increased the sample size would have increased the power, but also increased the variance, which would have made it more difficult to get accurate power and statistical significance.

Initially the data was reviewed for missing information, skew, kurtosis, and outliers. A complete data set would have contained 300 images, five images for each well. However in experiment 5, there was no third replica for fractal 4, consequently there were 295 images for analysis.

One of the assumptions of the statistical tests is that the data is normal as indicated by skew and kurtosis numbers greater than or less than zero. The skew and kurtosis of the raw data was severe for all dependent variables, in which case a data

transformation is recommended, see table 1. Two different transformations were compared, 1/x and LOG10(x+C). LOG10(x+C) was most effective at improving skew and kurtosis of the data, table 1. The chosen correction factor (C) was 1, which is recommend when there is data with a zero value so that taking the log is possible [42]. After skew and kurtosis were corrected close to normal, outliers were identified.

Table 2: Skew and Kurtosis for Dependent Variables Before and After Transformation.

	Raw Skew	Post Log 10 Skew	Raw Kurtosis	Post Log 10 Kurtosis
Neurons	2.150	-.882	8.002	.823
Dendrites/Neuron	2.745	.051	10.175	-1.034
Clumps	2.639	.803	8.069	-.499
Dendrites/Clump	3.192	1.186	12.199	.113

The Raw Skew and Raw Kurtosis scores indicate that the raw data did not fit a normal curve. The Post Log 10 Skew and Post Log 10 Kurtosis indicate that after adding a correction (1) to the raw data and taking the log, the data more closely fit a normal curve with close to 0 for skew and kurtosis.

Outliers were identified by reviewing the z score of the dependent variables and box plots. "Using Multivariate Statistics" suggests that in larger data sets, standardized scores (z score) greater than 3.29 are univariate outliers [42]. This analysis was conducted and there were only two outliers in dendrites per clump variable. Outliers were looked for in the box plots of the dependent variables, table 2. There were many more outliers identified for all dependent variables using this method of analysis. However, the recommended methods of dealing with these outliers is to delete them if they are believed to be wrong or miss-entered, change the data to the next point above (or below) it, or do a transformation to pull them closer to the center. The outlier data was believed to be correct so it was not deleted, it was not changed because that did not seem to be in keeping with the observations of the experiments and it would have meant changing an observation of zero neurons to the next higher number which seemed misleading. The data had already been transformed so it there was no further action taken on the outliers.

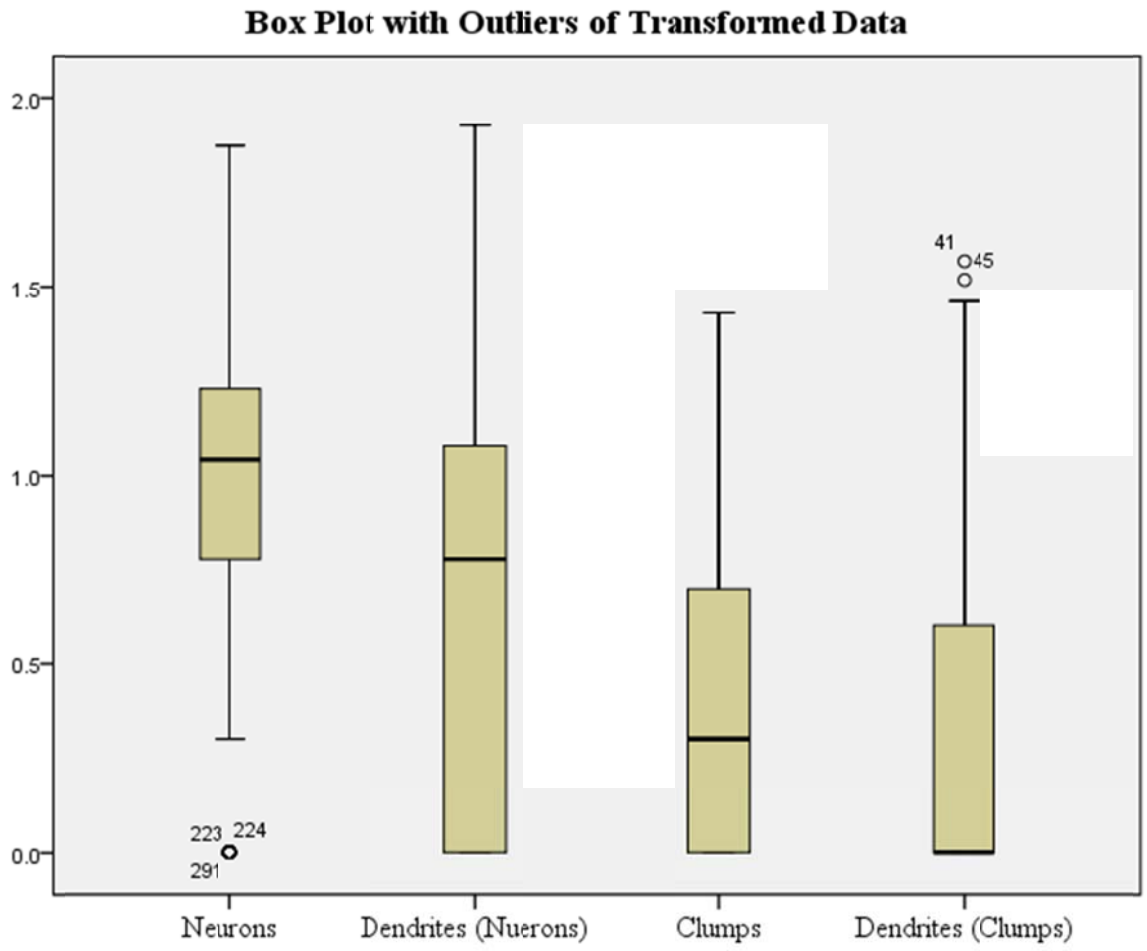

Figure 16: Box Plot with Outliers of Transformed Data. The figure shows that outliers were left unadjusted for the statistical tests because the standardized scores were within the recommended range for the size of the data set and it would have meant changing the zero neuron observations which was decided against.

In addition the data was checked specifically for multivariate outliers using Mahalanobis D^2. The Mahalanobis D^2 were computed with regression and then the probability of those scores was checked through the use of a chi-squared analysis [43]. There were five data points that had an unusual combination of variables. The outliers came from experiments 2 (three outliers) and experiment 4 (two outliers) and each outlier came from a different well in the experiment. The raw data for each of the outliers was

checked and the readings for each dependent variable seemed reasonable. Because there was no pattern to the outliers and because there were so few, no additional action was taken.

Once the data was transformed to fit a normal curve and outliers were identified and considered, in order to determine what effect the fractals had on the dependent variables, a MANCOVA was used. A multivariate model was selected because there were several dependent variables analyzed in the experiment. MANOVA/MANCOVA's work best when dependent variables are negatively correlated and are worst when dependent variables are highly correlated or not correlated at all [42]. When dependent variables are moderately correlated the data is well suited for a MANOVA/MANCOVA [42]. Table 3 contains the correlation for the dependent variables. The lowest correlation was .140 between neurons and dendrites (clumps), and the highest correlation was .725 between clumps and dendrites (clumps). The strongest correlation between neurons and dendrites (neurons) was .629. Healthy cells should have synapses with neighboring cells and if the cell adhesion is improved to sustain healthier neurons this correlation should become stronger.

Table 3: Dependent Variable Correlation.

	Neurons	Dendrites (Neurons)	Clumps	Dendrites (Clumps)
Neurons	1	.629	.213	.140
Dendrites (Neurons)	.629	1	.333	.364
Clumps	.213	.333	1	.725
Dendrites (Clumps)	.140	.364	.725	1

Table 3 shows the correlation table used Pearson and a two tailed test. The correlations are neither too close, nor too far apart to use a MANOVA and MANCOVA.

Over the course of the trials it was noted that the viability of the cells varied based on lot number. Due to this observation, a MANCOVA test with lot number as a covariate was performed to determine if lot number had an effect on the dependent variables. The MANCOVA revealed that lot number did significantly affect the dependent variables ($\alpha \leq .001$, $\beta \geq .993$). However, the fractal design had a statistically significant effect on neuron growth with or without the covariate and because of this; the variability between lot numbers did not appear to have a negative effect on the experiment. If the use of the covariate had been required to obtain statistical significance of the fractal then future experiments might consider the use of more lot numbers. The fractal design had a significant effect on the neurons and dendrites (neurons) ($\alpha \leq .01$), a statistically significant effect on dendrites on clumps ($\alpha = .046$), and no significant effect on clumps. However, the observed power for the fractal effect on the dependent variables was only greater than .80 for the neurons and dendrites (neurons) ($\beta = .950$, $\beta = .977$), consequently only the post hoc tests for neurons and dendrites (neurons) have enough power to be assured that a type II error was not made, table 4.

Table 4: MANCOVA Results for Tests of Between-Subjects Effects.

Source		df	Mean Square	F	Sig.	Observed Power[e]
Corrected Model	Neurons	4	1.015	7.259	.000	.996
	Dendrites(Neurons)	4	2.733	11.804	.000	1.000
	Clumps	4	.939	6.338	.000	.989
	Dendrites (Clumps)	4	2.287	15.563	.000	1.000
Intercept	Neurons	1	17.320	123.853	.000	1.000
	Dendrites(Neurons)	1	37.816	163.306	.000	1.000
	Clumps	1	13.385	90.379	.000	1.000
	Dendrites (Clumps)	1	18.368	124.998	.000	1.000
Lot Num	Neurons	1	1.683	12.038	.001	.933
	Dendrites(Neurons)	1	5.889	25.431	.000	.999
	Clumps	1	3.152	21.283	.000	.996
	Dendrites (Clumps)	1	7.922	53.910	.000	1.000
Fractal	Neurons	3	.812	5.806	.001	.950
	Dendrites(Neurons)	3	1.585	6.846	.000	.977
	Clumps	3	.213	1.438	.232	.380
	Dendrites (Clumps)	3	.396	2.693	.046	.652

Table 4 shows the results from the MANCOVA and illustrates that the Lot Number had a statistically significant effect on all dependent variables. The Fractal had a statistically significant effect on neurons and dendrites on neurons when taking both significance and observed power into consideration.

In addition to the MANCOVA test, a Bonferroni post hoc test was performed to evaluate the effect the fractals had on the dependent variables. As previously mentioned, the observed power was not great enough to depend on the results for clumps and dendrites (clumps). The Bonferroni post hoc test for neurons and dendrites (neurons) which met the observed power requirements ($\beta \geq .80$) are in table 5. The statistically significant ($\alpha \leq .05$) results are highlighted in yellow.

Table 5: MANCOVA Fractal Pairwise Comparisons Using Bonferroni Post Hoc Test.

Dependent Variable	Fractal I	Fractal J	Mean Difference (I-J)	Std. Error	Sig.[b]	95% Confidence Interval for Difference[b] Lower Bound	95% Confidence Interval for Difference[b] Upper Bound
Neurons	3	4	-.111	.062	.458	-.276	.055
		7	-.131	.061	.198	-.293	.031
		9	.094	.061	.739	-.068	.257
	4	3	.111	.062	.458	-.055	.276
		7	-.020	.062	1.000	-.185	.145
		9	.205*	.062	.007	.040	.370
	7	3	.131	.061	.198	-.031	.293
		4	.020	.062	1.000	-.145	.185
		9	.225*	.061	.002	.063	.387
	9	3	-.094	.061	.739	-.257	.068
		4	-.205*	.062	.007	-.370	-.040
		7	-.225*	.061	.002	-.387	-.063
Dendrites (Neurons)	3	4	-.266*	.080	.006	-.479	-.054
		7	-.139	.079	.469	-.348	.070
		9	.065	.079	1.000	-.143	.274
	4	3	.266*	.080	.006	.054	.479
		7	.128	.080	.672	-.085	.340
		9	.332*	.080	.000	.119	.544
	7	3	.139	.079	.469	-.070	.348
		4	-.128	.080	.672	-.340	.085
		9	.204	.079	.059	-.004	.413
	9	3	-.065	.079	1.000	-.274	.143
		4	-.332*	.080	.000	-.544	-.119
		7	-.204	.079	.059	-.413	.004

Table 5 shows only pairwise comparison with greater than $\beta \geq .80$ are shown. Statistically significantly ($\alpha \leq .05$) pairwise comparisons in fractals are highlighted in yellow. F9 had the lowest neuronal growth, significant when compared with F4 and F7. F9 had the fewest dendrites, although only significant when compared with F4.

5.2.2 – Results

The results from the MANCOVA in table 4 provide valuable information on how to proceed in future bioreactor designs. The MANCOVA results reject and fail to reject different parts of the null hypothesis. There is a difference in neuron growth between F9 versus F4 and F9 versus F7. In both comparisons, F9 had fewer neurons than F4 and F7. With respect to dendrites (neurons) on fractals, there is a difference between F3 and F4 and between F9 and F4. F4 had greater dendrites than both F3 and F9. The MANCOVA fails to reject other parts of the null hypothesis. With this in mind, future bioreactor designs should aim for a density similar to F4 and use caution in excessively dense patterns as seen in F9, figure 1.

Chapter 6 – DISCUSSION

The results from the qualitative and quantitative analysis provide several areas to consider during the next phase of developing a brain bioreactor. The two primary areas for improvement from the qualitative assessment are reducing clumping neurons both when plating and over the course of the experiment and the difficulty in preventing the neurons from falling off the fractal, points 2 and 5 respectively. In regards to clumping, the cells had healthier looking synapses at DIV 7 when compared to DIV 11, figures 11 and 12 which is an indicator of poor adhesion to the plate. According to the BrainBits fact page, the primary cause of clumping is poor preparation of the substrate with PDL (PLL in this experiment) [44]. However, as previously mentioned PLL has been used successfully in long term cell culture [27]. The BrainBits FAQ page states that hypothetically there is a difference in PLL and PDL, however they have found little difference [40, 45]. While the use of PLL was a departure from protocol, there are several supporting documents that suggest the use of PLL would not have resulted in the observed clusters. It is possible that there is a better cell adhesion mediator for titanium than PDL. A review on neuronal cell adhesion, conducted by Roach et al. recognized the tendency for neurons to clump up after 7 DIV when using PLL and suggested the use of alternate cell adhesion methods such as laminin, fibroconnectin, or polyethyleneimine (PEI) [46]. It should also be noted that there is sparse information regarding neuronal growth on titanium, only one paper was identified during a literature search, and it is likely that the ideal cell adhesion mediator for titanium has yet to be identified. Future

work with titanium substrate should begin with comparing different cell adhesion mediators to identify one better suited than PLL/PDL for long term neuronal cell culture.

The second area that needs to be addressed for the next phase of the brain bioreactor is increasing the amount of neurons that are seeded on the fractal surface. Although the neurons grew on all sides of the fractal, many of them fell off the fractal surface and remained in the bottom of the well, figure 15. The next generation of brain bioreactor needs to incorporate channels so that the neurons have no choice but to remain on the fractal surface. The bioreactor will be able to be filled with a small amount of media and neurons and the neurons will have a better chance of equaling distributing along the surface. The channels will also provide vertically aligned surface for the neurons to grow in the y direction for 3D growth as well as provide more control over neuron placement.

Lastly, the results from the analysis of variances conducted indicated that for most fractals, the fractal pattern did not influence the number of neurons or dendrites per neuron. The growth on F9 was statistically less (α = .007, .002) when compared to F4 and F7, respectively. Comparing the pattern of F4, F7, and F9 in figure 1, F9 has more densely arranged branches than F4 and F7. Future bioreactor designs should avoid placing the branches too closely together. It should also be recognize that future bioreactor designs that utilize a more effective CAM and incorporate channels should improve cell viability and provide more consistent results during the analysis.

Despite the shortcomings of the first generation bioreactor, this research provides the ground work for the next phase of MEMs based free standing scaffolds for neural

tissue engineering. The fractal design is more aligned with the innate branching in neural networks and this is the first fractal based scaffold to be evaluated. This is also one of the few free standing scaffolds to be evaluated in neural tissue engineering as most designs have shallow surface features and remain connected to the wafer. Finally, this is also the first work that evaluated the biocompatibility of titanium thin film deposition and neuronal growth elucidating that the titanium coating is biocompatible even when coated on a non-biocompatible structure (SU8-100). The next generation of brain bioreactor will incorporate the findings found within this work to create a more robust and accurate brain bioreactor.

REFERENCES

1. Dale Purves, G.J.A., David Fitzpatrick, William C. Hall, Anthony-Samual LaMantia, Leonard E. White, ed. *Neuroscience*. 5 ed., ed. G.J.A. Dale Purves, David Fitzpatrick, William C. Hall, Anthony-Samual LaMantia, Leonard E. White. 2012, Sinauer Associates, Inc.: Sunderland, Massachusetts.
2. Organization, W.H. *World Health Organization*. 2007 [cited 2013 05/09/13]; Available from: http://www.who.int/mediacentre/news/releases/2007/pr04/en/.
3. Center, N.N.S.C.I.S. *NSCISC National Spinal Cord Injury Statistical Center* 2007 [cited 2013 05/09/15]; Available from: https://www.nscisc.uab.edu/.
4. Cullen, D.K., et al., *Neural tissue engineering and biohybridized microsystems for neurobiological investigation in vitro (Part 1).* Critical Reviews™ in Biomedical Engineering, 2011. **39**(3).
5. Wang, M., et al., *Bioengineered scaffolds for spinal cord repair.* Tissue Engineering Part B: Reviews, 2011. **17**(3): p. 177-194.
6. Wrobel, M.R. and H.G. Sundararaghavan, *Directed migration in neural tissue engineering.* Tissue Engineering Part B: Reviews, 2013. **20**(2): p. 93-105.
7. Schroeder, M.R., *Fractals, chaos, power laws: Minutes from an infinite paradise*. 2012: Courier Corporation.
8. TeÂl, T., *Fractals, multifractals and thermodynamics: an introductory review.* Z. Naturforsch, 1988.

9. Kiselev, V.G., K.R. Hahn, and D.P. Auer, *Is the brain cortex a fractal?* Neuroimage, 2003. **20**(3): p. 1765-1774.

10. Wikipedia. *Fractal Dimension*. 2013 [cited 2013 18/09/13]; Available from: http://en.wikipedia.org/wiki/Fractal_dimension.

11. Fernández, E. and H.F. Jelinek, *Use of fractal theory in neuroscience: methods, advantages, and potential problems.* Methods, 2001. **24**(4): p. 309-321.

12. Díaz Lantada, A., et al., *Fractals in tissue engineering: toward biomimetic cell-culture matrices, microsystems and microstructured implants.* Expert review of medical devices, 2013. **10**(5): p. 629-648.

13. Pakkenberg, B. and H.J.G. Gundersen, *Neocortical neuron number in humans: Effect of sex and age.* Journal of Comparative Neurology, 1997. **384**(2): p. 312-320.

14. Ribeiro, F.M., et al., *Animal models of neurodegenerative diseases.* Revista Brasileira de Psiquiatria, 2013. **35**(2): p. S82-S91.

15. Jucker, M., *The benefits and limitations of animal models for translational research in neurodegenerative diseases.* Nature medicine, 2010. **16**(11): p. 1210-1214.

16. Rowe, L., et al., *Active 3-D microscaffold system with fluid perfusion for culturing in vitro neuronal networks.* Lab on a chip, 2007. **7**(4): p. 475.

17. Gurkan, U.A., et al., *Simple Precision Creation of Digitally Specified, Spatially Heterogeneous, Engineered Tissue Architectures.* Advanced Materials, 2013. **25**(8): p. 1192-1198.

18. Tang-Schomer, M.D., et al., *Bioengineered functional brain-like cortical tissue.* Proceedings of the National Academy of Sciences, 2014. **111**(38): p. 13811-13816.

19. Hanni, H., *Development of Fractal and Electrode Eomponents for Organotypic Culture in a Novel Three-Dimensional Bioreactor System*, in *Electrical Engineering*. 2011, Wayne State Univeresity. p. 73.

20. Nguyen, L., S. Hippenmeyer, and I. ebrary, *Cellular and molecular control of neuronal migration*. Vol. 800; 800. 2014, Dordrecht: Springer.

21. McAllister, A.K., *Cellular and molecular mechanisms of dendrite growth.* Cerebral cortex (New York, N.Y.: 1991), 2000. **10**(10): p. 963-973.

22. Miller, F.D. and D.R. Kaplan, *Signaling mechanisms underlying dendrite formation.* Current opinion in neurobiology, 2003. **13**(3): p. 391-398.

23. Dent, E.W., S.L. Gupton, and F.B. Gertler, *The growth cone cytoskeleton in axon outgrowth and guidance.* Cold Spring Harbor perspectives in biology U6 - ctx_ver=Z39.88-2004&ctx_enc=info%3Aofi%2Fenc%3AUTF-8&rfr_id=info:sid/summon.serialssolutions.com&rft_val_fmt=info:ofi/fmt:kev:mtx:journal&rft.genre=article&rft.atitle=The+growth+cone+cytoskeleton+in+axon+outgrowth+and+guidance&rft.jtitle=Cold+Spring+Harbor+perspectives+in+biology&rft.au=Dent%2C+Erik+W&rft.au=Gupton%2C+Stephanie+L&rft.au=Gertler%2C+Frank+B&rft.date=2011-03-01&rft.eissn=1943-0264&rft.volume=3&rft.issue=3&rft_id=info:pmid/21106647&rft.externalDocID=21106647&paramdict=en-US U7 - Journal Article, 2011. **3**(3).

24. Davies, R.W. and B.J. Morris, *Molecular Biology of the Neuron*. Molecular and Cellular Neurobiology Series. 2004, Oxford: Oxford University Press.

25. Letourneau, P., Condic, M., & Snow, D., *Interactions of Developing Neurons with the Extracellular Matrix.* The Journal of Neuroscience, 1991. **14**(3): p. 13.

26. Hopkins, A.M., et al., *3D in vitro modeling of the central nervous system.* Progress in Neurobiology, 2015. **125**(0): p. 1-25.

27. Kaech, S. and G. Banker, *Culturing hippocampal neurons.* Nature Protocols, 2006. **1**(5): p. 2406-2415.

28. *Adhesion of cells to surfaces coated with polylysine. Applications to electron microscopy.* The Journal of Cell Biology, 1975. **66**(1): p. 198-200.

29. Letourneau, P., *Possible Roles for Cell-to-Substratum Adhesion in Neuronal Morphogenesis.* Developmental Biology, 1975. **44**: p. 14.

30. Bacakova, L., et al., *Modulation of cell adhesion, proliferation and differentiation on materials designed for body implants.* Biotechnology Advances, 2011. **29**(6): p. 739-767.

31. Mukhopadhyay, S., J.P. Banerjee, and S.S. Roy, *Effects of liquid viscosity, surface wettability and channel geometry on capillary flow in SU8 based microfluidic devices.* International Journal of Adhesion and Adhesives, 2013. **42**(0): p. 30-35.

32. De Ville, M., et al., *Simple and low-cost fabrication of PDMS microfluidic round channels by surface-wetting parameters optimization.* Microfluidics and Nanofluidics, 2012. **12**(6): p. 953-961.

33. Nordström, M., et al., *Rendering SU-8 hydrophilic to facilitate use in micro channel fabrication.* Journal of Micromechanics and Microengineering, 2004. **14**(12): p. 1614-1617.

34. Vernekar, V.N., et al., *SU-8 2000 rendered cytocompatible for neuronal bioMEMS applications.* Journal of Biomedical Materials Research - Part A, 2009. **89**(1): p. 138-151.

35. Carballo-Vila, M., et al., *Titanium oxide as substrate for neural cell growth.* Journal of Biomedical Materials Research Part A, 2009. **90A**(1): p. 94-105.

36. Brors, D., et al., *Interaction of spiral ganglion neuron processes with alloplastic materials in vitro.* Hearing research, 2002. **167**(1-2): p. 110-121.

37. Chem, M. *NANO SU-8 Negative Tone Photoresist Formulations 50-100*. 2002 [cited 2015 25 June 2015]; Available from: http://www.microchem.com/pdf/SU8_50-100.pdf.

38. LifeTechnologies. *Isolation, Culture, and Characterization of Cortical and Hippocampal Neurons*. 2015 [cited 2015 6 July]; Available from: https://www.lifetechnologies.com/us/en/home/references/protocols/neurobiology/neurobiology-protocols/isolation-culture-and-characterization-of-cortical-and-hippocampal-neurons.html.

39. Balgude, A.P., et al., *Agarose gel stiffness determines rate of DRG neurite extension in 3D cultures.* Biomaterials, 2001. **22**(10): p. 1077-1084.

40. LLC, B. *BrainBits Dissociated Kit Primary Neuronal Plating Protocol*. 2015 [cited 2015 6 July]; Available from: http://www.brainbitsllc.com/dissociated-kit-primary-neuronal-plating-protocol/.

41. L, D. and H. S, *The MAP2/Tau family of microtubule-associated proteins.* Genome Biology [NLM - MEDLINE] U6 - ctx_ver=Z39.88-2004&ctx_enc=info%3Aofi%2Fenc%3AUTF-8&rfr_id=info:sid/summon.serialssolutions.com&rft_val_fmt=info:ofi/fmt:kev:mtx:journal&rft.genre=article&rft.atitle=The+MAP2%2FTau+family+of+microtubule-associated+proteins&rft.jtitle=Genome+Biology+%5BNLM+-+MEDLINE%5D&rft.au=Dehmelt+L&rft.au=Halpain+S&rft.date=2005-01-01&rft.eissn=1474-760X&rft.volume=6&rft.issue=1&rft.spage=204&rft.externalDocID=912450591&paramdict=en-US U7 - Journal Article, 2005. **6**(1): p. 204.

42. Tabachnick, B.G.F., Linda S., *Using Multivariate Statistics*. 5th ed, ed. S. Hartman. 2007, Boston, MA: Pearson Education, Inc. 980.

43. Pearson. *Analyses of Covariance*. 2015 [cited 2015 13 July 2015]; Available from: http://www.pearsonhighered.com/assets/hip/gb/uploads/Mayers_Intro_Stats_SPSS_Chapter_15.pdf.

44. LLC, B. *FAQ*. 2015 [cited 2015 8/07/15]; FAQ page on BrainBits website]. Available from: http://www.brainbitsllc.com/faq/.

45. Brewer, G.J. and C.W. Cotman, *Survival and growth of hippocampal neurons in defined medium at low density: advantages of a sandwich culture technique or low oxygen.* Brain research, 1989. **494**(1): p. 65-74.

46. Roach, P., et al., *Surface strategies for control of neuronal cell adhesion: A review.* Surface Science Reports, 2010. **65**(6): p. 145-173.

ABSTRACT

EVALUATION OF MEMS FABRICATED FRACTAL BASED FREE STANDING SCAFFOLDS FOR THE PURPOSES OF DEVELOPING A BRAIN BIOREACTOR

by

BRANDY BROADBENT

December 2015

Advisor: Dr. Gregory W. Auner

Major: Biomedical Engineering

Degree: Master of Science

The brain is the most complex organ in the body due to the multiple cell types, billions of tightly packed synapses, extracellular matrix, and intricate topography. Micro-electrical-mechanical fabrication techniques exhibit promise in the field of neuronal tissue engineering because the shape is highly controllable and a variety of materials can be used in creation of bioreactors. This work evaluates the ability of a free standing TiO_2 coated fractal scaffold to support healthy neuronal growth. Also evaluated is the propensity for the neurons to take advantage of the 3D growing surface without the use of complex extracellular matrix factors over the course of eleven days in vitro. The results indicate that while it is possible for neurons to grow on the MEMs fabricated fractal scaffold and grow in 3D, key adjustments to the scaffold and cell adhesion protein will better facilitate long term neuronal growth in future generations of the brain bioreactor.

AUTOBIOGRAPHICAL STATEMENT

My interest in science sparked as a high school student in Norman, OK and continued to grow as a biology major at the United States Air Force Academy in Colorado Springs, CO. While at the Academy I was introduced to the basics of a variety of engineering fields including mechanical, electrical, and aeronautical which started an interest in engineering. After graduation I spent nine and a half years fulfilling my military obligation by flying helicopters and serving in the Air Force. I learned to pilot one of the most technically advanced systems in the world, the HH-60G Pavehawk, which taught me to use and evaluate complex integrated systems such as rotors, transmission, engines, radar, and communication equipment.

The biomedical engineering program is a unique opportunity to combine my interests in science, engineering, and technology. I am particularly interested in neural engineering because there is so little known about the brain and how to address its complexities and much less is known about how to address its injuries and ailments. My experiences as a rescue pilot in Afghanistan and Iraq provided me with my first observations of the inadequacies of modern medicine when treating brain injuries and I hope that I can contribute to research that will help to improve the treatments.